High Degradation of Trichloroethylene in Water by Nanostructured MeNPs@CALB Biohybrid Catalysts

Noelia Losada-Garcia[iD], **Alba Rodriguez-Otero and Jose M. Palomo** *[iD]

Department of Biocatalysis, Institute of Catalysis (CSIC), Marie Curie 2, Cantoblanco, Campus UAM, 28049 Madrid, Spain; n.losada@csic.es (N.L.-G.); alba.rodriguez.96@gmail.com (A.R.-O.)
* Correspondence: josempalomo@icp.csic.es; Tel.: +34-9158-5476-8

Abstract: In this study, a methodology was developed for the rapid degradation of trichloroethylene (TCE) and 1,1-dichloroethylene (1,1-DCE) in distilled water and room temperature without the production of toxic chlorinated by-products. This process was carried out using bionanohybrids of different metals (Pd, Fe, Cu and Zn) obtained by enzyme–metal coordination called MeNPs@CALB, which present different metal species and nanoparticle sizes. The **Cu$_2$O@CALB** biohybrid, which contained Cu$_2$O nanoparticles, showed excellent catalytic performance in TCE degradation by removing 95% (>125 ppm) in 10 min using 1.5 g/L of catalyst. On the other hand, in the degradation reaction of 1,1-DCE, **Cu$_2$O@CALB** eliminated 94% (93 ppm) in 1 min. **Cu$_2$O@CALB** exhibited excellent stability and recyclability under sustainable conditions, maintaining its effectiveness in more than 90% for three cycles.

Keywords: trichloroethylene; catalytic degradation; metal bionanohybrid; groundwater remediation; green chemistry

1. Introduction

Volatile Chlorinated Organic Compounds (VCOCs) such as trichloroethylene (TCE) or 1,1-Dichloroethylene (DCE) have been widely used as solvents in heavy industries as a degreasing agent for metals (before the 1990s) [1] and electronic components, chemical intermediate [2] and dry-cleaning facilities [3]. Chlorinated organic compounds have been frequently found in subsurface environments as dense non-aqueous phase liquids (DNAPL) [4] and TCE is one of the most ubiquitous contaminants in soil and in contaminated groundwater [5] due to improper handling or accidental release during applications in industry [6].

The toxic and persistent nature of TCE poses a serious threat to the health of humans and ecological receptors and, for this reason, the treatment of waters contaminated with this compound must be adequately treated [7]. Trichloroethylene is classified as a Group 1 human carcinogen by the International Agency for Research on Cancer (IARC) [8]. According to the United States Environmental Protection Agency (EPA), the TCE and 1,1-DCE control standard is 0.0050 mg/L and 0.007 mg/L, respectively [9]. Today, the presence of chlorinated organic pollutants in groundwater has become the global ecological problem. Exposure of such pollutants threatens human health and can cause serious damage to the immune, nervous, and male systems [10]. Therefore, effective remediation and complete mineralization of TCE in aquifers is urgently required to reduce these effects [11].

In this context, the development of circular and holistic processes mimicking the biological life cycle, where every end is a new beginning, is crucial to achieving a more sustainable future. The design and implementation of competitive circular processes must integrate the biomimetic rationale to satisfy four essential criteria: simplicity, efficiency, cost-effectiveness, and material availability [12,13].

Different remediation approaches have been explored for the removal of TCE from contaminated sites, but attributed to the electronegative nature of chlorine substituents [14]; TCE is susceptible to transformation via reducing pathways [15]. Some of the methods used in the last decades include thermal incineration [16]; biodegradation [17]; phytoremediation [18]; physical adsorption [19]; advanced oxidation processes (AOP) such as photocatalytic oxidation [20]; Fenton oxidation methods [21]; and reductive methods dechlorination, such as zero valence reduction [22,23], catalytic [24,25], as well as electrochemical dechlorination methods [26], using zero-valent iron [27], palladium-based materials [28] and bimetallic metals [29]. Although these methods are effective for TCE degradation, each has its advantages and limitations due to the use of numerous oxidants in addition to heat treatment techniques, ultraviolet irradiation, as well as transition metals for the activation of oxidants [30].

In this work, a new methodology has been developed to degrade chlorinated toxic compounds in water (TCE, 1,1-DCE) in a simple, green and sustainable way through metal bionanohybrids (Pd, Fe, Cu and Zn) (Figure 1). Bionanohybrids present advantages compared with other metal systems because they are constituting of very small metal nanoparticles in a protein network which confers them high stability and they are located in a monodispersed way, which has been demonstrated to allow superior catalytic properties [31–33].
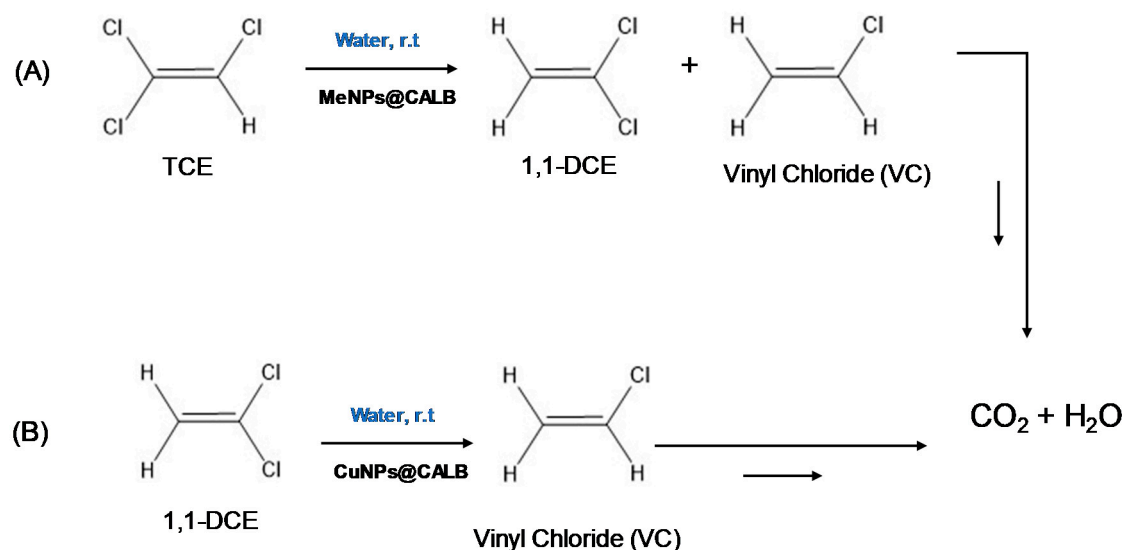

Figure 1. TCE degradation mechanism catalyzed by **MeNPs@CALB** biohybrid (**A**); 1,1-DCE degradation mechanism catalyzed by **CuNPs@CALB** biohybrid (**B**).

2. Results and Discussion

2.1. Trichloroethylene (TCE) Degradation Catalyzed by MeNPs@CALB Biohybrids

Different metal–enzyme bionanohybrids (**MeNPs@CALB)** of different metals (Pd, Fe, Cu or Zn) were prepared and characterized following protocols previously described (see Supporting information and Figure S1) [31–33].

The performance of the different heterogeneous metal biohybrids was evaluated as catalysts for the removal of TCE by means of their complete degradation in aqueous medium at room temperature and in some cases using 10 mM of a green oxidant such as H_2O_2 (33% *v/v*) (Table 1).

Table 1. Elimination of TCE catalyzed by **MeNPs@CALB** [a].

Entry	Catalyst	H_2O_2 (mM) [b]	Time (min)	Degradation Yield (%) [c]	Presence of Vinyl Chloride [d]	Degraded (mg L^{-1}) [e]
1	No catalyst	-	-	-	-	-
2	CALB	-	-	-	-	-
3	Pd(0)@CALB	0	5	85	no	112
4	$FeCO_3$@CALB	0	300	75	yes	99
5	Cu_2O@CALB	0	5	85	no	112
6	$Cu_3(PO_4)_2$@CALB	0	5	83	no	109
7	$Cu_3(PO_4)_2$@CALB1	0	5	67	no	9
8	$Cu_3(PO_4)_2$@CALB2	0	5	81	yes	106
9	$Cu_3(PO_4)_2$@CALB3	0	5	74	yes	97
10	Cu(0)@CALB	0	60	16	yes	21
11	ZnO@CALB	0	5	41	no	54
12	$FeCO_3$@CALB	10	420	>90	no	>119
13	Cu_2O@CALB	10	5	85	no	112
14	Cu(0)@CALB	10	5	78	yes	102
15	ZnO@CALB	10	5	85	yes	112

[a] TCE (1 mM), catalyst (3 mg), 2 mL solution (91% water, 9% ACN), 25 °C. [b] Amount of H_2O_2 (33% *v/v*). [c] The degradation yield of TCE was determined by HPLC. [d] Presence of vinyl chloride as sub-product <5%. [e] Amount of degraded TCE was determined by HPLC from the initial concentration (131.4 mg L^{-1}).

The reaction was carried out in aqueous media (91% distilled water, 9% ACN) at 25 °C. Initially, no oxidant was used in the reaction. No conversion was obtained without a catalyst or exclusively using the enzyme (Table 1, entries 1,2).

The **Pd(0)@CALB** and **Cu_2O@CALB** hybrids showed the best result, with 85% (112 ppm) of TCE degraded in 5 min (Table 1, entries 3 and 5), which *as far as we know* represents the fastest degradation process for TCE catalyzed by these metals [34,35]. The hybrid **$Cu_3(PO_4)_2$@CALB** showed a conversion of 83% (Table 1, entry 6), which shows that the Cu species have a strong influence on this reaction as a catalyst, being in these three cases without the production of toxic substances as by-products (VC).

In the case of iron, **$FeCO_3$@CALB** needed 300 min to achieve a conversion of 75% (entry 4). In other copper species such as $Cu_3(PO_4)_2$, lower conversion was obtained for the same reaction time. Furthermore, in the case of **$Cu_3(PO_4)_2$@CALB2** and **$Cu_3(PO_4)_2$@CALB3** (entries 8,9), vinyl chloride was found after the reaction was stopped. The hybrid containing Cu (0) species showed moderate conversion (20%) even after 60 min conversion, founding also the presence of vinyl chloride (entry 10).

This degradation process was also studied by adding hydrogen peroxide as a green oxidant, as mentioned above, for those cases where the degradation reaction was very slow (Table 1, entries 12–15) or in the case of **Cu_2O@CALB**, to see the effect that it produced (entries 5 and 13). The presence of the green oxidant did not show any effect on **Cu_2O@CALB**, having the same degradation value in both cases, while in other hybrids of different metals such as **$FeCO_3$@CALB** or **ZnO@CALB**, improvements in the degradation yields were obtained (Table 1, entries 12 and 15). In particular, in the case of **$FeCO_3$@CALB**, in the presence of hydrogen peroxide, no presence of other peaks (such as vinyl chloride) was observed after stopping the reaction.

This may be due to the fact that in the case of **$FeCO_3$@CALB**, it presented a structure of nanorods with which the catalytic effectiveness is less. Despite this, better results were obtained with our Fe catalyst in comparison with the others described in the literature [36]. Furthermore, in the case of **ZnO@CALB**, the addition of hydrogen peroxide as an oxidant improved the degradation capacity of the catalyst from 41 to more than 80% in 5 min (Table 1, entries 11 and 15), which represent in both cases an improvement compared with other ZnO nanoparticles described in the literature [37].

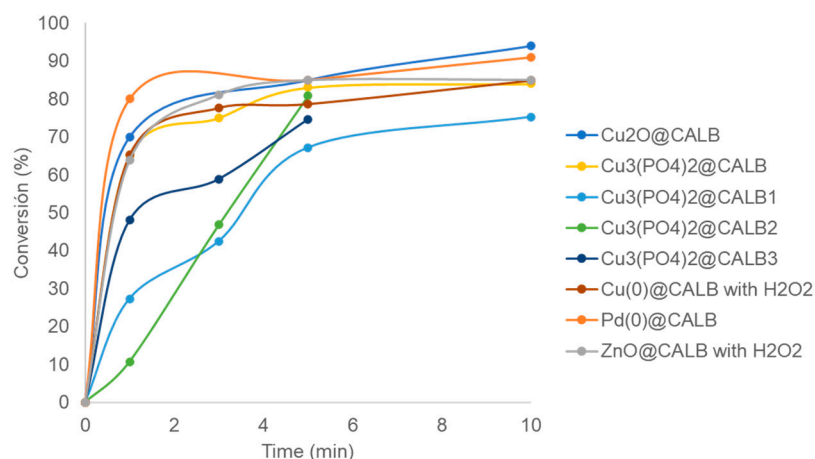Furthermore, the TCE degradation profile for different bionanohybrids was analyzed in the first 10 min (Figure 2).

Figure 2. TCE degradation reaction profile catalyzed by the different **MeNPs@CALB** biohybrids. Experimental conditions: [TCE]: 131.4 mg·L^{-1}, [H$_2$O$_2$]: 0 or 10 mM, water pure.

The results in Figure 2 showed that very rapid degradation was performed, where there was 95% or 125 ppm of TCE. The **Pd(0)@CALB** and **Cu$_3$(PO$_4$)$_2$@CALB** biohybrids showed similar profiles, although with a slightly lower percentage, 91% (119 ppm) and 84% (110 ppm), respectively. Using H$_2$O$_2$ as a green oxidant, we can see that **Cu(0)@CALB** and **ZnO@CALB** also present similar profiles although with values below 90%. These results demonstrate that the NPs of Cu$_2$O species are the best in catalytic performance for this reaction.

According to all these results, it was decided to choose the copper catalyst **Cu$_2$O@CALB** for further studies since this metal is cheaper, less toxic and therefore more sustainable than palladium.

2.2. Reuse of Cu$_2$O@CALB Biohybrid in the Degradation of TCE

Once optimal conditions were obtained, a recycling experiment was conducted using the best bionanohybrid, **Cu$_2$O@CALB** (Figure 3A). The catalyst exhibited excellent stability, maintaining almost 90% of the catalytic efficiency after three cycles of use. In order to evaluate the structure of the catalyst after the three cycles, XRD analysis was performed. Figure 3B shows that metal species of the catalyst (Cu$_2$O) have not changed after being used, which demonstrates the high stability of the bionanohybrid in this reaction.
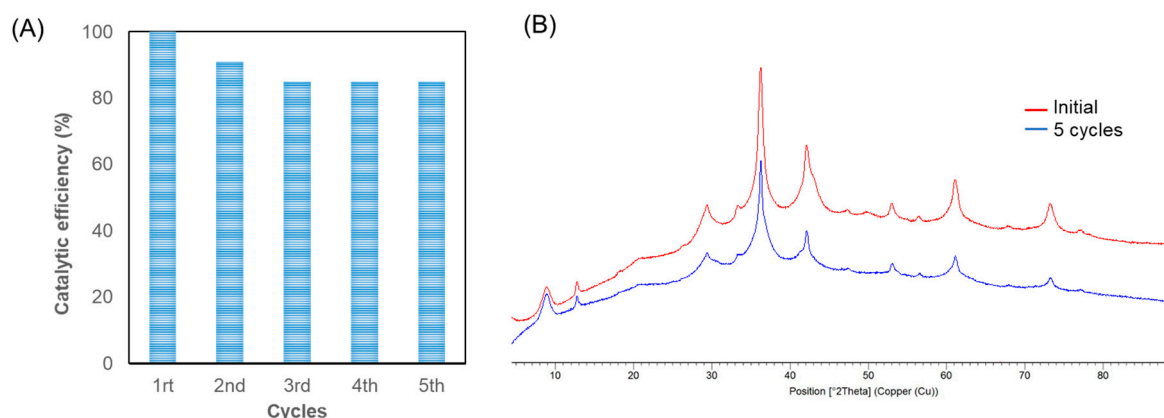

Figure 3. (**A**) Recycling of **Cu$_2$O@CALB** in oxidative degradation of TCE. Experimental conditions: [TCE]: 131.4 mg·L^{-1}, 2 mL aqueous solution (91% water, 9% ACN); (**B**) XRD spectra at the start of the reaction (red) and after three reaction cycles (blue).

2.3. 1,1-Dichloroethylene (1,1-DCE) Degradation Catalyzed by CuNPs@CALB Biohybrids

In order to broad the scope of applicability of these **CuNPs@CALB** biohybrids, the degradation of another toxic chlorinated compound was evaluated in optimal conditions. 1,1-Dichloroethylene (1,1-DCE) is found as a degradation product of tetrachloroethylene or perchloroethylene (PCE) and trichloroethylene (TCE), which like TCE has been studied as a powerful carcinogen. In fact, many studies have shown that DCE degradation is slower than that of TCE, making it a highly problematic by-product. In this section, the two most efficient bionanohybrids (**Cu$_2$O@CALB** and **Cu$_3$(PO$_4$)$_2$@CALB**) in the removal of TCE are applied, as can be seen in Table 2.

Table 2. Elimination of 1,1-DCE catalyzed by **CuNPs@CALB** biohybrids [a].

Bionanohybrid	Time (min) [b]	Yield (%) [c]	TOF (min^{-1}) [d]	DCE Degraded (mg L^{-1}) [e]
Cu$_2$O@CALB	1	93.5	233.8	92.5
Cu$_3$(PO$_4$)$_2$@CALB	1	91.5	228.6	90.5

[a] 1,1-DCE (1mM), catalyst (3 mg), 2.2 mL solution (91% water, 9% ACN), 25 °C. [b] Time of reaction (min). [c] Yield of reaction in the degradation of TCE was determined by HPLC. [d] Turn over frequency (TOF) [mmols TCE converted/mmols of metal × time (min)$^{-1}$]. [e] Amount of degraded 1,1-DCE was determined by HPLC from the initial concentration (98.96 mg·L^{-1}).

In this case, >90% degradation of DCE was observed after 1 min in both cases, the best results coming from using **Cu$_2$O@CALB** as catalysts with almost 94% degradation (Table 2). This shows the high catalytic effectiveness of copper nanoparticles with different species (Cu(I) and Cu(II)), obtaining an excellent result in degradation more than 90 ppm of the organic pollutant.

3. Materials and Methods

3.1. Materials

Lipase B from *Candida antarctica* (CALB) solution (Lipozyme® CALB) was purchased from Novozymes (Copenhagen, Denmark). Copper (II) sulphate pentahydrate [Cu$_2$SO$_4$·5H$_2$O] and hydrogen peroxide (33%) were from Panreac (Barcelona, Spain). [(NH$_4$)$_2$Fe(SO$_4$)$_2$] (Mohr's salt), Zinc sulphate heptahydrate [ZnSO$_4$·7H$_2$O], palladium acetate [Pd(OAc)$_2$], sodium bicarbonate, sodium phosphate, sodium borohydride, trichloroethylene (TCE), 1,1-dichloroethylene (1,1-DCE), and vinyl chloride were purchased from Sigma-Aldrich (St. Louis, MO, USA).

3.2. General Synthesis of MeNPs@CAL-B Biohybrids

Bionanohybrids with different metals were synthesized, such as palladium (Pd), iron (Fe), copper (Cu), and zinc (Zn). The iron, copper and palladium bionanohybrids were described in previous publications [31–33], except for the synthesis and characterization of the zinc catalyst.

3.2.1. Synthesis and Characterization of FeCO$_3$@CAL-B Biohybrids

1.8 mL of commercial (18 mg of protein) Lipozyme® CALB solution was added to 60 mL buffer 0.2M sodium bicarbonate pH = 10 in a 100 mL glass bottle containing a small magnetic bar stirrer. Then 600 mg of (NH$_4$)$_2$Fe(SO$_4$)$_2$ (10 mg/ml) was added to the protein solution and it was maintained for 16 hours at room temperature stirring at 380 r.p.m. After the first 30 min incubation, the solution turned cloudy (greenish gray) and the pH solution was measured indicating a decrease from 10 to 8. After 16 h incubation, the solid was recovered and re-suspended in 15 mL of water or treated with NaBH$_4$ (300 mg dissolved in 6 mL of water added in two times of 3 mL) incubated at 15 min and then recovered and re-suspended in 15 mL of water. Then in all cases solid was washed with distilled water (15 mL × 3). In the case of previous use of borohydride, the pH of the final washing water

must be around 5 to avoid residues of sodium borohydride and its interaction with the freeze-drying. Finally, the supernatant was removed and the pellet of each falcon was re-suspended in 2 mL of water, collected in a cryotube, frozen with liquid nitrogen and lyophilized for 16 hours. The catalyst so called $FeCO_3$@CALB was obtained.

ICP-OES analysis revealed that this bionanohybrid contained 47% (weight) of iron. XRD analysis of the solid showed the presence of iron (II) carbonate (siderite, $FeCO_3$) as the iron species (Figure S1). TEM analysis confirmed the formation of nanorods ($FeCO_3$NRs) with a size of approximately 7 nm diameter × 59 nm length induced by the protein matrix (Figure S1B).

3.2.2. Synthesis and Characterization of CuNPs@CAL-B Biohybrids

1.8 mL of commercial (18 mg of protein) Lipozyme® CALB solution was added to 60 mL buffer 0.1 M sodium bicarbonate pH = 10 in a 250 mL glass bottle containing a small magnetic bar stirrer. Then, 600 mg of $Cu_2SO_4\cdot5H_2O$ (10 mg/mL) was added to the protein solution and it was maintained for 16 h. After the first 30 min incubation, the solution turned cloudy (turquoise) and the pH solution was measured, indicating a decrease to 8 pH value depending on the buffer used. After 16 h, 6 mL of $NaBH_4$ (300 mg) aqueous solution (1.2 M) was added to the cloudy solution (in two times of 3 mL) obtaining a final concentration of 0.12 M of sodium borohydride in the mixture. The solution turned rapidly black and the mixture was reduced during the 30 min. After the incubation, the mixture was centrifuged at 8000 rpm for 5 min, (10 mL per falcon type tube). The generated pellet was re-suspended in 15 mL of water. The pH of the supernatant solution was measured to be approximately 9. It was centrifuged again at 8000 rpm for 5 min and the supernatant removed. The pH of the supernatant solution was measured again, and given a pH value of 7. The process was repeated twice more. Finally, the supernatant was removed and the pellet of each falcon was re-suspended in 2 mL of water, all solutions were collected in a round-bottom flask, frozen with liquid nitrogen, and lyophilized for 16 h. After that, 150 mg of the so called Cu(0)@CALB was obtained. ICP-OES analysis revealed that this bionanohybrid contained 84% (weight) of copper (Table S1). XRD analysis of the solid showed the presence of Cu(0) and a minor pike of Cu_2O was found (Figure S1). TEM analysis confirmed the formation of nanoparticles with a size of 9 nm in diameter (Figure S1).

Another variation of the protocol was used in these cases with 0.1 M of buffer sodium phosphate, in which the reduction step was not performed, obtaining $Cu_3(PO_4)_2$@CALB. ICP-OES analysis revealed that this bionanohybrid contained 32% (weight) of copper (Table S1). XRD pattern showed peaks distribution observed in corresponding to the $Cu(PO_4)_3$ species (Figure S1). However, in this case, TEM analysis revealed the formation of smaller crystalline spherical nanoparticles of about 3 nm (Figure S1).

In addition to the last variation, an oxidation step was also performed instead of a reduction step by the addition of either 6 mL of a 500 mM solution of sodium hydroxide (NaOH) for 30 min or 6 mL of a 0.1 M solution of hydrogen peroxide (H_2O_2) for 30 min (60 μL of the H_2O_2 stock solution in 6 mL of distillate water), obtaining $Cu_3(PO_4)_2$@CALB1 and $Cu_3(PO_4)_2$@CALB2, respectively. ICP-OES analysis revealed that these bionanohybrids contained 35% and 22% (weight) of copper respectively. (Table S1). The copper species was conserved and spherical nanoparticles were also obtained of around 5–6 nm.

Different modifications of the phosphate protocol were made by changing the amount of enzyme. Initially, different bionanohybrids were prepared using double the amount of enzyme (3.6 mL CALB solution instead of 1.8 mL), obtaining Cu_2O@CALB. Also using phosphate method without the reducing step, an alternative protocol was performed using 18 mL of enzyme (10 times more than original protocol described above) and 72 h as synthetic time. It was called $Cu_3(PO_4)_2$@CALB3.

ICP-OES analysis revealed that these bionanohybrids contained 60% and 50% (weight) of copper respectively (Table S1). The copper species was conserved and spherical nanoparticles were also obtained for around 6 nm in the case of Cu_2O@CALB; and in the other SEM analysis, the formation of well-formed nanoflowers was revealed.

3.2.3. Synthesis and Characterization of Pd(0)@CAL-B Biohybrids

Pd(OAc)$_2$ (50 mg) were dissolved in 10 mL of MeOH. This solution was added to 40 mL of a distilled water solution containing 16 mg of CALB protein (1.6 mL of commercial Lipozyme® CALB solution of 10 mg protein/mL). The final solution was kept under gentle magnetic stirring for 24 h at room temperature. After that, the resulting suspension was separated by centrifugation (10,000 rpm; 4 °C; 15 min). The recovered pellet was washed once with 10 mL of distilled water containing 20% (*v/v*) of MeOH and twice with distilled water (2 × 10 mL). After this, the suspension was directly lyophilized to obtain catalyst in powder for later use. This solid was called Pd(0)@CALB.

ICP-OES analysis revealed that around 23% (*w/w*) of Pd was entrapped on the protein during the aggregation process (Table S1). XRD and XPS analysis of the solid showed the presence of Pd(0) carbonate was found (Figure S1). Scanning electron microscopy (SEM) revealed an aggregate with a mesoporous amorphous superstructure (Figure S1) composed by palladium atoms dispersed into an organic matrix (enzyme). TEM analysis confirmed the formation of nanoparticles with a size of around 2–7 nm in diameter (Figure S1).

3.2.4. Synthesis and Characterization of ZnO@CAL-B Biohybrids

1.8 mL of commercial (18 mg of protein) Lipozyme® CALB solution was added to 60 mL buffer 0.1 M of sodium bicarbonate pH = 10 in a 250 mL glass bottle containing a small magnetic bar stirrer. Then, 600 mg of ZnSO$_4$·7H$_2$O (10 mg / mL) was added to the protein solution and maintained for 16 h. After that, 6 mL of NaBH$_4$ (300 mg) aqueous solution (1.2 M) was added and after 30 min the mixture was centrifuged and pellet washed with water, frozen and lyophilized for 16 h. After that, the so called ZnO@CALB was obtained.

ICP-OES analysis revealed that this new bionanohybrid contained 36% (weight) of zinc (Table S1). XRD analysis of the solid showed the presence of Zinc oxide (ZnO) as the main zinc species (Figure S1). Scanning electron microscopy (SEM) revealed an aggregate with a mesoporous amorphous superstructure (Figure S1). TEM analysis confirmed the formation of nanoparticles with a size of around 5 nm in diameter (Figure S1).

3.3. Characterization Techniques

Inductively coupled plasma-optical emission spectrometry (ICP-OES) was performed on an OPTIMA 2100 DV instrument (PerkinElmer, Waltham, MA, USA). X-Ray diffraction (XRD) patterns were obtained using a Texture Analysis D8 Advance Diffractometer (Bruker, Billerica, MA, USA) with Cu Kα radiation. Transmission electron microscopy (TEM) images were obtained on a 2100F microscope (JEOL, Tokyo, Japan).

3.4. MeNPs@CALB Biohybrids Catalyzing the Degradation of Trichloroethylene (TCE)

A solution of 10 mM of TCE in pure acetonitrile was prepared; 0.2 mL of this solution was dissolved in 2 mL of distilled water to achieve a concentration of 1 mM TCE (131.4 mg·L^{-1}). Then, hydrogen peroxide (33% *v/v*) was added to this TCE solution to obtain a concentration 10 mM (2 μL H$_2$O$_2$ in 2 mL). To initialize the reaction, 3 mg of the catalyst (in case of Pd, 1 mg) was added to 2 mL of this solution (TCE and H$_2$O$_2$) in a 7 mL glass flask. Gentle stirring was provided at room temperature (25 °C) by a roller. For each degradation group, three parallel experiments were performed, and the error range was <5%. The TCE degradation yield was determined by HPLC analysis.

The HPLC analysis was performed in a JASCO HPLC equipment, a HPLC pump PU-4180 coupled with a UV-4075 UV-Vis detector. The analysis conditions were performed using a Kromasil–C8 (150 × 4.6 mm and 5 μm), at a flow of 1.0 mL/min; and a mobile phase: 50% (*v/v*) ACN in MilliQ water, with UV detector at λ = 215 nm. Before injection, 20 μL of sample were diluted in 180 μL of acetonitrile. Under these conditions, the retention time of TCE was 9 min. TCE sub-products such as 1,1-DCE

or vinyl chloride were identified at 7 min and 4 min, respectively, using commercial standard pure products of both substrates as control.

TOF (turnover frequency) value was calculated by [mmols TCE converted/mmols Cu $\times$ time $(min)^{-1}$].

3.5. Reuse of Cu₂O@CALB Biohybrid in the Degradation of TCE

The **Cu₂O@CALB** biohybrid was reused in five cycles for the degradation of TCE using the same experimental conditions described above. After each reaction cycle, the catalyst was washed with water several times, centrifuged and separated before the next reaction. In addition, XRD was performed on the sample after the five cycles to compare the chemical structure with that of the catalyst before the reaction.

3.6. MeNPs@CALB Biohybrids Catalyzing the Degradation of 1,1-Dichloroethylene (1,1-DCE)

A solution of 10 mM of 1,1-DCE in pure acetonitrile was prepared; 0.2 mL of this solution was dissolved in 2 mL of distilled water to achieve a concentration of 1 mM 1,1-DCE (98.96 mg·L^{-1}). To initialize the reaction, 3 mg of the catalyst was added to 2 mL of this solution in a 7 mL glass flask. Gentle stirring was provided at room temperature (25 °C) by a roller. At given time intervals, 20 μL of reaction solution was taken and diluted in 180 μL of acetonitrile pure for HPLC analysis. For each degradation group, three parallel experiments were performed, and the error range was <5%. HPLC conditions were the same as described above for TCE. Under these conditions, the retention time of 1,1-DCE was 7 min. The 1,1-DCE sub-products such as vinyl chloride were detected at 4 min, using commercial standard pure products of both substrates as control.

4. Conclusions

We have developed a fast, sustainable and efficient method to remove chlorinated compounds (TCE and 1,1-DCE) by direct degradation using enzyme-metal hybrids as heterogeneous catalysts.

The degradation reactions were carried out efficiently using water as a green solvent at room temperature. Here we have demonstrated the role of metal species in the effectiveness of target reactions, with Cu₂O nanoparticles being the best option among the different metal biohybrids synthesized since it was able to eliminate more than 95% of TCE (125 ppm) in 10 min with 3 mg of catalyst. In addition to degrading almost 94% of 1,1-DCE (93 ppm) in 1 min.

The successful evaluation of the scope of the reaction and the excellent recyclability observed for this catalyst open the possibility of expanding the application of these Cu nanocatalysts in environmental technology in the degradation of other toxic organic pollutants.

References

1. Chiu, W.A.; Jinot, J.; Scott, C.S.; Makris, S.L.; Cooper, G.S.; Dzubow, R.C.; Bale, A.S.; Evans, M.V.; Guyton, K.Z.; Keshava, N.; et al. Human health effects of trichloroethylene: Key findings and scientific issues. *Environ. Health Perspect.* **2013**, *121*, 303–311. [CrossRef]

2. Kueper, B.H.; Stroo, H.F.; Vogel, C.M.; Ward, C.H. Source zone remediation: The state of the practice. In *Chlorinated Solvent Source Zone Remediation*; Springer: New York, NY, USA, 2014; pp. 1–27.

3. Palau, J.; Marchesi, M.; Chambon, J.C.C.; Aravena, R.; Canals, A.; Binning, P.J.; Bjerg, P.L.; Otero, N.; Soler, A. Multi-isotope (carbon and chlorine) analysis for fingerprinting and site characterization at a fractured bedrock aquifer contaminated by chlorinated ethenes. *Sci. Total Environ.* **2014**, *475*, 61–70. [CrossRef]

4. Cucciniello, R.; Intiso, A.; Siciliano, T.; Palomares, A.E.; Martínez-Triguero, J.; Cerrillo, J.L.; Proto, A.; Rossi, F. Oxidative Degradation of Trichloroethylene over Fe_2O_3-doped Mayenite: Chlorine Poisoning Mitigation and Improved Catalytic Performance. *Catalysts* **2019**, *9*, 747. [CrossRef]

5. Zhang, M.; Dong, J. Phase-transfer catalysis enhanced remediation of trichloroethylene polluted groundwater by potassium permanganate. *Environ. Technol.* **2019**, 1–12. [CrossRef]

6. Liu, B.; Zhang, H.; Lu, Q.; Li, G.; Zhang, F. A CuNi bimetallic cathode with nanostructured copper array for enhanced hydrodechlorination of trichloroethylene (TCE). *Sci. Total Environ.* **2018**, *635*, 1417–1425. [CrossRef]

7. Tsai, T.T.; Kao, C.M.; Surampalli, R.Y.; Weng, C.H.; Liang, S.H. Treatment of TCE contaminated groundwater using fenton-like oxidation activated with basic oxygen furnace slag. *J. Environ. Eng.* **2010**, *136*, 288–294. [CrossRef]

8. International Agency for Research on Cancer. *IARC Monographs on the Identification of Carcinogenic Hazards to Humans*; World Health Organization: Geneva, Switzerland, 2019.

9. US Environmental Protection Agency. *Edition of the Drinking Water Standards and Health Advisories*; EPA 822-R-18-001; EPA Office of Water: Washington, DC, USA, 2018.

10. Danish, M.; Gu, X.; Lu, S.; Brusseau, M.L.; Ahmad, A.; Naqvi, M.; Farooq, U.; Zaman, W.Q.; Fu, X.; Miao, Z. An efficient catalytic degradation of trichloroethene in a percarbonate system catalyzed by ultra-fine heterogeneous zeolite supported zero valent iron-nickel bimetallic composite. *Appl. Catal. A Gen.* **2017**, *531*, 177–186. [CrossRef]

11. Yan, J.; Qian, L.; Gao, W.; Chen, Y.; Ouyang, D.; Chen, M. Enhanced Fenton-like degradation of trichloroethylene by hydrogen peroxide activated with nanoscale zero valent iron loaded on biochar. *Sci. Rep.* **2017**, *7*, 43051. [CrossRef]

12. Keijer, T.; Bakker, V.; Slootweg, J.C. Circular chemistry to enable a circular economy. *Nat. Chem.* **2019**, *11*, 190–195. [CrossRef]

13. Serrá, A.; Artal, R.; García-Amorós, J.; Sepúlveda, B.; Gómez, E.; Nogués, J.; Philippe, L. Hybrid Ni@ZnO@ZnS-Microalgae for Circular Economy: A Smart Route to the Efficient Integration of Solar Photocatalytic Water Decontamination and Bioethanol Production. *Adv. Sci.* **2020**, *7*, 1902447. [CrossRef]

14. Gonzalez-Olmos, R.; Anfruns, A.; Aguirre, N.V.; Masaguer, V.; Concheso, A.; Montes-Morán, M.A. Use of by-products from integrated steel plants as catalysts for the removal of trichloroethylene from groundwater. *Chemosphere* **2018**, *213*, 164–171. [CrossRef]

15. Mao, X.; Ciblak, A.; Baek, K.; Amiri, M.; Loch-Caruso, R.; Alshawabkeh, A.N. Optimization of electrochemical dechlorination of trichloroethylene in reducing electrolytes. *Water Res.* **2012**, *46*, 1847–1857. [CrossRef]

16. Huang, B.; Lei, C.; Wei, C.; Zeng, G. Chlorinated volatile organic compounds (Cl-VOCs) in environment sources, potential human health impacts, and current remediation technologies. *Environ. Int.* **2014**, *71*, 118–138. [CrossRef]

17. Li, J.; de Toledo, R.A.; Shim, H. Multivariate optimization for the simultaneous bioremoval of BTEX and chlorinated aliphatic hydrocarbons by *Pseudomonas plecoglossicida*. *J. Hazard. Mater.* **2017**, *321*, 238–246. [CrossRef]

18. Wang, C.; Ma, X.; Walsh, M.P. Competitive uptake and phytomonitoring of chlorinated contaminant mixtures by Redosier dogwood (*Cornus sericea*). *Int. J. Phytoremediat.* **2011**, *13*, 333–344. [CrossRef]

19. Xin, J.; Zheng, X.; Han, J.; Shao, H.; Kolditz, O. Remediation of trichloroethylene by xanthan gum-coated microscale zero valent iron (XG-mZVI) in groundwater: Effects of geochemical constituents. *Chem. Eng. J.* **2015**, *271*, 164–172. [CrossRef]

20. Biyoghe Bi Ndong, L.; Ibondou, M.P.; Gu, X.; Lu, S.; Qiu, Z.; Sui, Q.; Mbadinga, S.M. Enhanced photocatalytic activity of TiO$_2$ nanosheets by doping with Cu for chlorinated solvent pollutants degradation. *Ind. Eng. Chem. Res.* **2014**, *53*, 1368–1376. [CrossRef]

21. Liu, Y.; Zhou, A.; Gan, Y.; Li, X. Effects of inorganic anions on carbon isotope fractionation during Fenton-like degradation of trichloroethene. *J. Hazard. Mater.* **2016**, *308*, 187–191. [CrossRef]

22. Ahn, J.Y.; Kim, C.; Kim, H.S.; Hwang, K.Y.; Hwang, I. Effects of oxidants on in situ treatment of a DNAPL source by nanoscale zero-valent iron: A field study. *Water Res.* **2016**, *107*, 57–65. [CrossRef]

23. Han, Y.; Yan, W. Reductive dechlorination of trichloroethene by zero-valent iron nanoparticles: Reactivity enhancement through sulfidation treatment. *Environ. Sci. Technol.* **2016**, *50*, 12992–13001. [CrossRef] [PubMed]

24. Srebowata, A.; Tarach, K.; Girman, V.; Góra-Marek, K. Catalytic removal of trichloroethylene from water over palladium loaded microporous and hierarchical zeolites. *Appl. Catal. B Environ.* **2016**, *181*, 550–560. [CrossRef]

25. Yu, X.; Wu, T.; Yang, X.J.; Xu, J.; Auzam, J.; Semiat, R.; Han, Y.F. Degradation of trichloroethylene by hydrodechlorination using formic acid as hydrogen source over supported Pd catalysts. *J. Hazard. Mater.* **2016**, *305*, 178–189. [CrossRef] [PubMed]

26. Rajic, L.; Fallahpour, N.; Podlaha, E.; Alshawabkeh, A. The influence of cathode material on electrochemical degradation of trichloroethylene in aqueous solution. *Chemosphere* **2016**, *147*, 98–104. [CrossRef]

27. Lu, Q.; Jeen, S.W.; Gui, L.; Gillham, R.W. Nitrate reduction and its effects on trichloroethylene degradation by granular iron. *Water Res.* **2017**, *112*, 48–57. [CrossRef]

28. Han, Y.; Liu, C.; Horita, J.; Yan, W. Trichloroethene hydrodechlorination by Pd-Fe bimetallic nanoparticles: Solute-induced catalyst deactivation analyzed by carbon isotope fractionation. *Appl. Catal. B Environ.* **2016**, *188*, 77–86. [CrossRef]

29. Kumar, M.A.; Bae, S.; Han, S.; Chang, Y.; Lee, W. Reductive dechlorination of trichloroethylene by polyvinylpyrrolidone stabilized nanoscale zerovalent iron particles with Ni. *J. Hazard. Mater.* **2017**, *340*, 399–406. [CrossRef]

30. Shan, A.; Farooq, U.; Lyu, S.; Zaman, W.Q.; Abbas, Z.; Ali, M.; Idress, A.; Tang, P.; Li, M.; Sun, Y.; et al. Efficient removal of trichloroethylene in surfactant amended solution by nano Fe0-Nickel bimetallic composite activated sodium persulfate process. *Chem. Eng. J.* **2020**, *386*, 123995. [CrossRef]

31. Benavente, R.; Lopez-Tejedor, D.; Palomo, J.M. Synthesis of a superparamagnetic ultrathin FeCO$_3$ nanorods–enzyme bionanohybrid as a novel heterogeneous catalyst. *Chem. Commun.* **2018**, *54*, 6256–6259. [CrossRef]

32. Losada-García, N.; Rodríguez-Otero, A.; Palomo, J.M. Tailorable synthesis of heterogeneous enzyme–copper nanobiohybrids and their application in the selective oxidation of benzene to phenol. *Catal. Sci. Technol.* **2020**, *10*, 196–206. [CrossRef]

33. Cuenca, T.; Filice, M.; Palomo, J.M. Palladium nanoparticles enzyme aggregate (PANEA) as efficientcatalyst for Suzuki–Miyaura reaction in aqueous media. *Enzym. Microb. Technol.* **2017**, *95*, 242–247. [CrossRef]

34. Wang, X.; Wang, W.; Lowry, G.; Li, X.; Guo, Y.; Li, T. Preparation of palladized carbon nanotubes encapsulated iron composites: Highly efficient dechlorination for trichloroethylene and low corrosion of nanoiron. *R. Soc. Open Sci.* **2018**, *5*, 172242. [CrossRef] [PubMed]

35. Vargas, D.X.; De la Rosa, J.R.; Lucio-Ortiz, C.J.; Hernández-Ramirez, A.; Gerardo, A.; Flores-Escamilla, G.A.; Garcia, C.D. Photocatalytic degradation of trichloroethylene in a continuous annular reactor using Cu-doped TiO2 catalysts by sol–gel synthesis. *Appl. Catal. B Environ.* **2015**, *179*, 249–261. [CrossRef]

36. Li, F.; Vipulanandan, C.; Mohanty, K.K. Microemulsion and solution approaches to nanoparticle iron production for degradation of trichloroethylene. *Colloids Surf. A Physicochem. Eng. Asp.* **2003**, *223*, 103–112. [CrossRef]

37. Jang, D.G.; Ahn, C.H.; Choi, J.S.; Kim, J.H.; Kim, J.K.; Joo, J.C. Enhanced Removal of Trichloroethylene in Water Using Nano-ZnO/Polybutadiene Rubber Composites. *Catalysts* **2016**, *6*, 152. [CrossRef]